States in ^{205}Pb excited via the ^{204}Pb(d,p) reaction. II. The "particle" states*

C. F. Maguire,† D. G. Kovar,‡ W. D. Callender, § and C. K. Bockelman
Wright Nuclear Structure Laboratory, Yale University, New Haven, Connecticut 06520
(Received 8 December 1975; revised manuscript received 26 July 1976)

The higher-lying states in ^{205}Pb ($E_x \geq 2.57$ MeV) are examined by means of the ^{204}Pb(d,p) transfer reaction at incident energies of 13.0 and 20.0 MeV. In order to extract a reliable set of spectroscopic factors, a consistent set of distorted-wave Born approximation parameters is derived from analyses of new ^{208}Pb(d,p) data at $E_d = 13.0$ MeV, and by reanalysis of earlier ^{206,208}Pb(d,p) data. By avoiding proton optical parameters based on data in an energy region later found to contain resonances, and by using a deuteron potential which corrects for deuteron breakup, ^{208}Pb(d,p) spectroscopic factors consistent to ±15% are obtained. The improved distorted-wave Born approximation parameters are used to assign orbital angular momentum (l_n) values to a majority of 110 new levels in ^{205}Pb, most of them heretofore unknown. Significant fractions of the $1i_{11/2}$ and the $1j_{15/2}$, and the majority of the $2g_{9/2}$, $3d_{5/2}$, $4s_{1/2}$, $2g_{7/2}$, and $3d_{3/2}$ single-particle strengths are located. These strengths are found to be concentrated about the energy centroids. A previous theoretical calculation of spectroscopic strengths compares poorly with the experimental values.

[NUCLEAR REACTIONS ^{204}Pb(d,p), $E_x \geq 2.56$ MeV, $E_d = 13.0$ and 20.0 MeV, also ^{208}Pb(d,p), $E_d = 13.0$ MeV; measured $\sigma(E_p,\theta)$, extracted S_{lj}. Earlier ^{208}Pb(d,p) experiments at $E_d = 18.7$, 20.0, and 24.8 MeV and ^{206}Pb(d,p) at $E_d = 17.0$ MeV reanalyzed. ^{205}Pb results compared to weak-coupling theory.]

I. INTRODUCTION

The proton elastic excitation functions characteristic of the $A \approx 208$ region all show a striking similarity of structure between ~14.5 and ~17.5 MeV incident energy.[1,2] As illustrated in Fig. 1, these excitation functions consistently show resonances at approximately the same proton energies, independent of the particular nucleus being bombarded. It is now well known[3] that these resonances correspond to unbound states in the $A+1$ nucleus which are isobaric analogs of bound states in the parent nucleus. In particular, the energy spacings of the resonances lead to the interpretation of the bound states as the core A coupled to a neutron in one after another of the $N=6$ major shell orbitals. In the case of an even A target (0^+ g.s.) these excitations present a window, albeit a cloudy one, on the distribution of the shell-model single-particle strength in the adjacent odd nucleus. The extraction of nuclear structure information from these excitation functions is complicated by the interference of the resonance amplitudes with the direct background.[4] Nonetheless, the persistence and similarity of the resonance behavior suggests that the distribution of neutron single-particle strength is similar for the single-particle orbits in these odd nuclei.

This nuclear structure information is, of course, immediately available by means of the (d,p) reaction which directly populates the bound states according to their spectroscopic strengths. For example, the ^{206}Pb$(d,p)^{207}$Pb reaction has been studied by Moyer, Cohen, and Diehl.[5] Their analysis confirms that the higher-lying states populated in ^{207}Pb ($E_x > 2.7$ MeV) do indeed have the bunching of single-particle strength expected from the resonance study. The fact that fragmentation occurs is a reflection of a residual interaction between the neutron and the core. One is then led to ask what is the simplest residual interaction capable of predicting the observed spectrum? Evidence has been presented for a weak-coupling model explanation in the case of ^{207}Pb.[6] While a similar calculation has been performed for ^{205}Pb,[7] heretofore the existing experimental data have been insufficient for an adequate assessment of the model's success. The present work removes this obstacle and provides a stimulus for more refined theoretical analysis.

We report here the result of a series of ^{204}Pb$(d,p)^{205}$Pb experiments performed at 13.0 and 20.0 MeV incident deuteron energy. The states to be discussed are between 2.565 and 5.623 MeV in excitation and are fragments of the neutron single-particle states appearing in ^{209}Pb. A total of 110 levels are established and most of them are assigned a spin and spectroscopic strength. The ^{208}Pb$(d,p)^{209}$Pb reaction was also performed at the same incident energies for the purpose of normal-

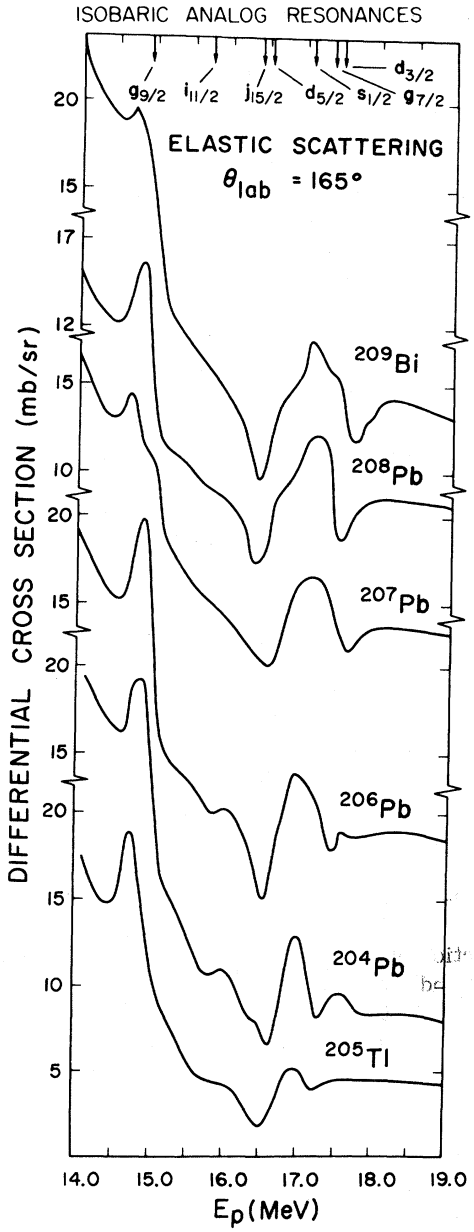

FIG. 1. Proton elastic excitation functions from six targets in the lead region showing the isobaric analog resonances (Ref. 1).

izing the ^{205}Pb spectroscopic factors to those of ^{209}Pb, with the intent of bypassing uncertainties inherent in the conventional distorted-wave Born approximation (DWBA) procedure.

Initially the bypass procedure was viewed as an important means of obtaining more accurate spectroscopic factors for ^{205}Pb. Although a variety of experiments clearly show that (except for the $1j_{15/2}$ orbital) the single-particle states in ^{209}Pb are very pure, in his survey of the ^{208}Pb$(d,p)^{209}$Pb studies, Macfarlane[8] found that the extracted (absolute) spectroscopic factors were consistent to no better than 25%. Since the ^{208}Pb$(d,p)^{209}$Pb is the single-nucleon transfer experiment closest to the idealization inherent in the conventional theoretical DWBA treatment, Macfarlane's figure of 25% has been widely quoted as representing the practical upper limit on the accuracy of that formalism. However, that conclusion was based on a set of disjoint analyses performed by different experimental teams, employing differing assumptions and a variety of optical potentials to extract the spectroscopic factors quoted by Macfarlane. Clearly a self-consistent analysis of the complete set of data is required. We have therefore reanalyzed all the experiments in the deuteron energy range 17.0–24.8 MeV, and are convinced, as a result, that the DWBA method is actually more reliable than the analyses surveyed by Macfarlane suggest.

The main problem in the earlier analyses lay with the choice of the proton parameters, and, to a lesser degree, with the deuteron breakup in the nuclear field of the target. The optical model does not apply in the lead region for protons in the range of $E_p = 14.5 - 17.5$ MeV because of the analog resonances shown in Fig. 1. Equally important, even when the protons are above the resonance region, it is improper to use an optical parameter set derived in the resonance region. However, one such proton parameter set, derived by Perey[9] in 1964, has received wide use in the analysis of direct reactions in the Pb nuclei, including one of the studies[10] used by Macfarlane.[8] We have avoided use of this proton potential, preferring the parameters recommended by Satchler.[11] These parameters also take into account the effects of deuteron break up.[12–14] With them we are able to obtain generally improved fits to the ^{209}Pb angular distributions, and a much more consistent set of ^{209}Pb spectroscopic factors than previously reported.[8] We believe that our use of the same optical-model treatment leads also to a consistent set of spectroscopic factors for ^{205}Pb.

II. ^{205}Pb EXPERIMENTAL SPECTRUM

The experimental apparatus has been described in the preceding paper. The experiments mentioned therein also contain data for the higher-lying states. In addition, several more experiments were undertaken specifically searching for these higher-lying states, involving exposures of 2500 and 4200 μC, respectively, at 13.0 MeV, and 735 μC at 20.0 MeV incident deuteron energies. This additional series of experiments achieved energy resolutions of approximately 7.0 keV for

the 13.0 MeV data, and 12.0 keV for the 20.0 MeV data.

The complete (d,p) spectrum of ^{205}Pb at $E_d = 20.0$ MeV is shown in Fig. 2. There is observed to be a tremendous increase in the magnitude and density of excitation starting at 2.56 MeV, a phenomenon simply explained by the shell model. In this interpretation the stripped neutron is able to populate an orbital only to the extent that it is unoccupied in the ^{204}Pb ground-state wave function. In the zero-order shell limit all the orbitals in the $N=6$ major shell (see Fig. 1 of the preceding paper) are completely empty in the ^{204}Pb ground state. On the other hand, the four holes in the $N=5$ major shell are expected to deplete only the $3p_{1/2}$ and the $2f_{5/2}$ subshells to any significant extent. The remaining orbitals in the $N=5$ major shell should be nearly completely full. Hence, in the simplest picture there is only a small amplitude for populating the three-hole configurations in ^{205}Pb, while the one-particle four-hole states should be excited to the full sum-rule limit.

The particle-state region of the ^{205}Pb spectrum is shown in more detail in Fig. 3. Considering the density of states, especially above 4.3 MeV excitation, it was not obvious that this experimental spectrum could be completely analyzed. With this in mind, the spectrum was resolved at each observation angle and at each energy independently. The spectrum analysis program AUTOFIT,[15] modified to become operator interactive, was used to decompose the often overlapping groups. This phase of the analysis has been described at length elsewhere.[16] It was found that at *all angles* and at *both* incident deuteron energies, the total spectrum could be fitted with the same number of levels at the same excitation energies. This crucial point is convincing because the 13.0 MeV data have better absolute energy resolution than do the 20.0 MeV data, yet there was no necessity to introduce additional levels to fit the 13.0 MeV spectrum.

Between 2.565 and 5.623 MeV of excitation, 110 levels of ^{205}Pb were definitely excited, most of them previously unknown. Their energies and position uncertainties are listed in Table I. An analysis of the energy determination procedure leads us to believe that between the first and last states of Table I, there could be a ±10 keV systematic error attributed to magnetic field variations and calibration uncertainties. With respect to its nearby neighbors, the relative position of each state is known much better. It is these local position uncertainties (i.e., within a window of about 200 keV) which are recorded in the ΔE_x column of Table I. Between 5.62 and 5.75 MeV a few (<10) states are weakly populated, but are too closely spaced to be resolved. Between 5.75 and 6.73 MeV, no states could be discerned above the background (in this region the background is ~10 μb/sr per 3 keV channel at $E_d = 13.0$ MeV). The extraction of the spectroscopic factors merits discussion next.

III. OPTICAL-MODEL PARAMETERS; ^{208}Pd$(d,p)^{209}$Pb

The usual method of direct-reaction analysis involves a comparison of the angular distributions predicted by a DWBA code such as DWUCK[17] with

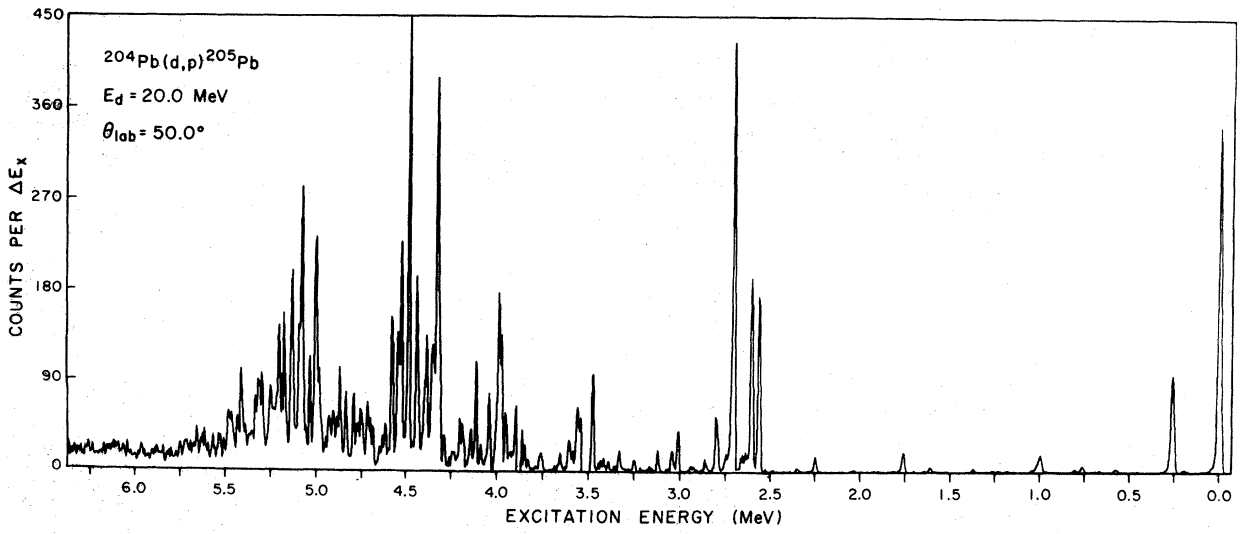

FIG. 2. The (d,p) spectrum of ^{205}Pb at 20.0 MeV incident energy. The figure is derived from two separate exposures of 10 200 and 735 μC for the low-lying and the higher-lying states, respectively.

those extracted from the experiment. In the present case, a direct comparison of the experimental shapes to those predicted by the DWBA is not entirely necessary: the cross section calculation can be bypassed to a large extent by using the ^{208}Pb$(d,p)^{209}$Pb single-particle angular distributions as templates for the ^{204}Pb$(d,p)^{205}$Pb analysis.

Precise deuteron scattering cross sections from ^{204}Pb and ^{208}Pb have been reported by Ungrin *et al.*[18] using 13.1 MeV incident energy deuterons. With their values we are able to obtain spectroscopic factors in ^{205}Pb normalized to the corresponding strengths in ^{209}Pb. Successive (d,p) exposures were made on ^{204}Pb and ^{208}Pb targets. A solid-state monitor at $\theta_{lab} = 75°$ detected the elastically scattered deuterons during both runs. The outgoing proton groups from ^{205}Pb and ^{209}Pb were recorded on separate photographic plates. For a state in ^{205}Pb with the same spin and parity as a given single-particle state in ^{209}Pb, it is straight forward to show that the ratio of spectroscopic factors is:

$$\frac{S_{lj}^{205}}{S_{lj}^{209}} = \frac{N_{lj}(205)}{N_{lj}(209)} \frac{\sigma_d(204)}{\sigma_d(208)} \frac{N_d(208)}{N_d(204)}. \quad (1)$$

$N_{lj}(A+1)$ is the number of proton events corresponding to excitation of the $^{A+1}$Pb level; $\sigma_d(A)$ is the elastic deuteron cross section from ^{A}Pb at the monitor angle (75°); $N_d(A)$ is the number of elastic deuteron monitor counts during the ^{A}Pb(d,p) run; and A is either 204 or 208.

This equation is independent of the target thicknesses involved and assumes only equal Q values to the residual states of ^{205}Pb and ^{209}Pb. Should these Q values be different, a correction factor, the ratio of the intrinsic DWBA cross sections $[\sigma_{lj}^{DW}(209)/\sigma_{lj}^{DW}(205)]$, must be introduced to the right-hand side of Eq. (1). Effectively this procedure removes the uncertainties associated with the choice of optical-model parameter sets. A complete bypassing of the reaction calculation is

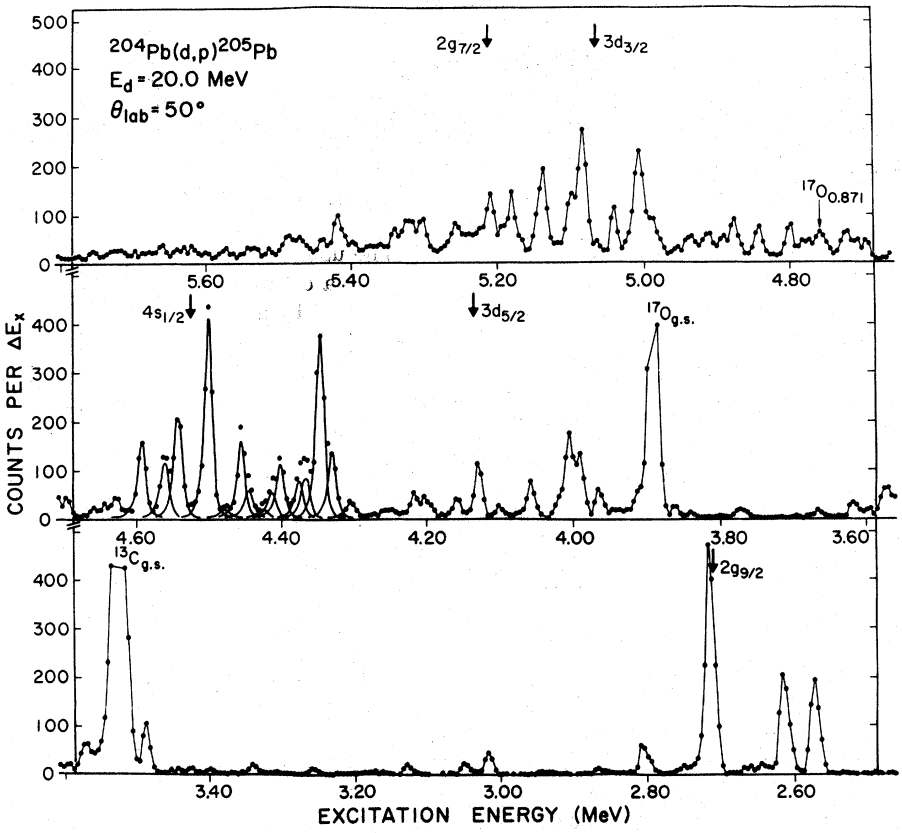

FIG. 3. A sample of the decomposition accomplished by the peak analysis program AUTOFIT for one of the 20.0 MeV spectra. The overlapping lines around 4.5 MeV of excitation are those produced by the program, while elsewhere the data points are connected to guide the eye. Arrows indicate the centroids of the single-particle strengths in ^{205}Pb.

TABLE I. The single-particle fragments in ^{205}Pb.

No.	Ex. energy	ΔE_x	nlj	S_{lj}	ΔS_{lj}
1	2.565	···	$2g_{9/2}$	0.16	±0.01
2	2.607	±0.001	$2g_{9/2}$	0.18	±0.01
3	2.634	±0.003	$(2g_{9/2})$	(0.017)	±(0.002)
4	2.657	±0.003	$(2g_{9/2})$	(0.013)	±(0.002)
5	2.708	±0.001	$2g_{9/2}$	0.38	±0.02
6	2.798	±0.002	$2g_{9/2}$	0.05	±0.003
7	2.862	±0.002	$(2g_{9/2})$	(0.009)	±(0.002)
8	2.931	±0.002	$2g_{9/2}$	0.005	±0.001
9	3.010	±0.002	$2g_{9/2}$	0.030	±0.002
10	3.043	±0.002	$2g_{9/2}$	0.015	±0.002
11	3.119	±0.002	$2g_{9/2}$	0.016	±0.002
12	3.165	±0.003	$(2g_{9/2})$	(0.005)	±(0.001)
13	3.249	±0.003	$(3d_{5/2})$	(0.006)	±(0.001)
14	3.306	±0.003	$(2g_{9/2})$	(0.008)	±(0.002)
15	3.334	±0.002	$(3d_{5/2})$	(0.006)	±(0.001)
16	3.393	±0.003	$1i_{11/2}$	0.09	±0.02
17	3.422	±0.004	$1i_{11/2}$	0.03	±0.006
18	3.435	±0.002	$(3d_{5/2})$	(0.006)	±(0.001)
19	3.483	±0.002	$3d_{5/2}$	0.045	±0.002
20	3.511	±0.002	$1i_{11/2}$	0.20	±0.02
21	3.533	±0.002	$3d_{5/2}$	0.022	±0.001
22	3.566	±0.002	$3d_{5/2}$	0.023	±0.001
23	3.592	±0.004	$l \geq 4$		
24	3.613	±0.003	$1i_{11/2}$	0.06	±0.01
25	3.659	±0.002	$3d_{5/2}$	0.009	±0.001
26	3.764	±0.002	$3d_{5/2}$	0.009	±0.002
27	3.834	±0.004		$\sigma_{max} = 20\mu b/sr$ [a]	
28	3.857	±0.002	$3d_{5/2}$	0.007	±0.002
29	3.889	±0.004		$\sigma_{max} = 35\ \mu b/sr$	
30	3.950	±0.003	$(3d_{5/2})$	(0.005)	(±0.001)
31	3.961	±0.002	$3d_{5/2}$	0.024	±0.003
32	3.988	±0.002	$3d_{5/2}$	0.055	±0.005
33	4.002	±0.002	$1j_{15/2}$	0.38	±0.05
34	4.016	±0.003	$(3d_{5/2})$	(0.001)	(±0.0003)
35	4.055	±0.003	$3d_{5/2}$	0.028	±0.003
36	4.074	±0.003	$l \geq 4$	$\sigma_{max} = 35\ \mu b/sr$	
37	4.097	±0.002	$3d_{5/2}$	0.009	±0.002
38	4.127	±0.002	$3d_{5/2}$	0.050	±0.005
39	4.156	±0.002	$3d_{5/2}$	0.014	±0.002
40	4.187	±0.004	$(4s_{1/2})$	(0.002)	±(0.0004)
41	4.199	±0.003	$(4s_{1/2})$	(0.004)	±(0.0008)
42	4.214	±0.002	$3d_{5/2}$	0.019	±0.002
43	4.239	±0.003	$(3d_{5/2})$	(0.005)	(±0.001)
44	4.254	±0.003	$3d_{5/2}$	0.008	±0.002
45	4.299	±0.002	$3d_{5/2}$	0.015	±0.002
46	4.326	±0.002	$3d_{5/2}$	0.049	±0.007
47	4.342	±0.002	$3d_{5/2}$	0.145	±0.022
48	4.361	±0.002	$3d_{5/2}$	0.035	±0.005
49	4.372	±0.002	$3d_{5/2}$	0.035	±0.005
50	4.389	±0.002	$3d_{5/2}$	0.042	±0.006
51	4.412	±0.002	$3d_{5/2}$	0.025	±0.004
52	4.428	±0.004	$(3d_{5/2})$	(0.006)	(±0.001)
53	4.443	±0.003	$3d_{5/2}$	0.020	±0.003
54	4.452	±0.002	$3d_{5/2}$	0.050	±0.008
55	4.497	±0.002	$4s_{1/2}$	0.340	±0.030
56	4.539	±0.002	$4s_{1/2}$	0.185	±0.020
57	4.558	±0.002	$4s_{1/2}$	0.100	±0.015
58	4.590	±0.002	$4s_{1/2}$	0.150	±0.020
59	4.624	±0.002	$(3d_{5/2}, 3d_{3/2})$	(0.016, 0.024)	(±0.003, 0.005)
60	4.642	±0.004	$(4s_{1/2})$	(0.021)	(±0.004)

TABLE I. *(continued)*

No.	Ex. energy	ΔE_x	nlj	S_{lj}	ΔS_{lj}
61	4.656	±0.005		$\sigma_{max} \leq 45$ μb/sr	
62	4.693	±0.003	$(2g_{7/2})$	(0.025)	(±0.005)
63	4.709	±0.003	$(3d_{5/2}, 3d_{3/2})$	(0.013, 0.020)	(±0.003, 0.004)
64	4.722	±0.002	$4s_{1/2}$	0.05	±0.010
65	4.745	±0.004		$\sigma_{max} \leq 50$ μb/sr	
66	4.760	±0.002	$3d_{3/2}$	0.014	±0.003
67	4.777	±0.002	$3d_{3/2}$	0.014	±0.003
68	4.787	±0.002	$3d_{3/2}$	0.011	±0.002
69	4.803	±0.002	$3d_{3/2}$	0.014	±0.003
70	4.840	±0.002	$2g_{7/2}$	0.055	±0.008
71	4.874	±0.002	$2g_{7/2}$	0.039	±0.007
72	4.913	±0.002	$3d_{3/2}$	0.028	±0.005
73	4.891	±0.002	$3d_{3/2}$	0.027	±0.005
74	4.936	±0.003	$2g_{7/2}$	0.035	±0.006
75	4.954	±0.003	$(3d_{3/2} + 2g_{7/2})$	(0.008 + 0.013)	(±0.002, 0.003)
76	4.978	±0.002	$3d_{3/2}$	0.025	±0.005
77	4.990	±0.002	$3d_{3/2}$	0.038	±0.006
78	5.004	±0.002	$3d_{3/2}$	0.120	±0.020
79	5.014	±0.003	$3d_{3/2}$	0.030	±0.006
80	5.040	±0.002	$3d_{3/2}$	0.040	±0.006
81	5.065	±0.002	$3d_{3/2}$	0.013	±0.003
82	5.083	±0.002	$3d_{3/2}$	0.145	±0.017
83	5.100	±0.003	$3d_{3/2}$	0.075	±0.011
84	5.120	±0.003	$3d_{3/2}$	0.018	±0.004
85	5.139	±0.002	$3d_{3/2}$	0.100	±0.015
86	5.167	±0.004	$(2g_{7/2})$	(0.017)	(±0.004)
87	5.180	±0.003	$3d_{3/2}$	0.065	±0.012
88	5.192	±0.003	$3d_{3/2}$	0.022	±0.004
89	5.209	±0.002	$3d_{3/2}$	0.076	±0.014
90	5.226	±0.004	$2g_{7/2}$	0.035	±0.007
91	5.242	±0.003	$2g_{7/2}$	0.033	±0.007
92	5.258	±0.002	$2g_{7/2} + 3d_{3/2}$		
93	5.285	±0.003	$2g_{7/2}$	0.017	±0.003
94	5.304	±0.002	$2g_{7/2}$	0.049	±0.007
95	5.317	±0.003	$2g_{7/2}$	0.038	±0.006
96	5.325	±0.002	$2g_{7/2}$	0.025	±0.005
97	5.344	±0.002	$2g_{7/2}$	0.039	±0.006
98	5.364	±0.004	$2g_{7/2}$	0.025	±0.005
99	5.378	±0.004	$(3d_{3/2})$	(0.017)	(±0.004)
100	5.399	±0.003	$(2g_{7/2})$	(0.013)	(±0.003)
101	5.418	±0.002	$2g_{7/2}$	0.056	±0.008
102	5.439	±0.002	$2g_{7/2}$	0.025	±0.005
103	5.452	±0.004	$2g_{7/2}$	0.020	±0.005
104	5.473	±0.003	$2g_{7/2}$	0.040	±0.008
105	5.486	±0.003	$2g_{7/2}$	0.036	±0.005
106	5.515	±0.004	$2g_{7/2}$	0.023	±0.005
107	5.534	±0.003	$2g_{7/2}$	0.027	±0.005
108	5.572	±0.003	$2g_{7/2}$	0.020	±0.004
109	5.598	±0.002	$(2g_{7/2})$	(0.010)	(±0.002)
110	5.623	±0.003	$2g_{7/2}$	0.020	(±0.004)

[a] Maximum cross sections are for 13.0 MeV incident energy.

not, however, possible. It will be seen that the single-particle centroids in ^{205}Pb are bound up to 300 keV more strongly than in ^{209}Pb. This fact necessitates the use of the direct-reaction theory to calculate the change in the cross section induced by the Q-value differential between ^{209}Pb and ^{205}Pb.

In Sec. I we have stated that the lack of consistency in spectroscopic factors in the Pb region noted by Macfarlane[8] is related to the use of a proton optical potential derived from proton data taken in a resonance region where the optical model is inapplicable. Other experiments[19] have relied on a global proton optical potential[20] which has been shown not to be applicable in the lead region.[9] We decided to reanalyze the previous ^{208}Pb$(d,p)^{209}$Pb data using a proton optical potential derived by Satchler.[11] In Figs. 4–6 we show the original and the reanalyzed fits to the experimental angular distributions for the ^{209}Pb single-particle states, including the 18.7 MeV data by Jeans *et al.*,[19] the 20.0 MeV data of Kovar *et al.*,[21] and the 24.8 MeV data of Muehllehner *et al.*[10] Moyer *et al.*[5] have done the ^{206}Pb$(d,p)^{207}$Pb experiment at 17.0 MeV, and have reported spectroscopic factors for the ^{209}Pb single-particle states based on a 2% ^{208}Pb impurity in their target. These spectroscopic factors were recalculated here by comparing the original and recalculated DWBA angular distributions. For completeness, we then show in Fig. 7 fits to the strongest fragments in ^{207}Pb. Finally, Fig. 8 displays new data on the

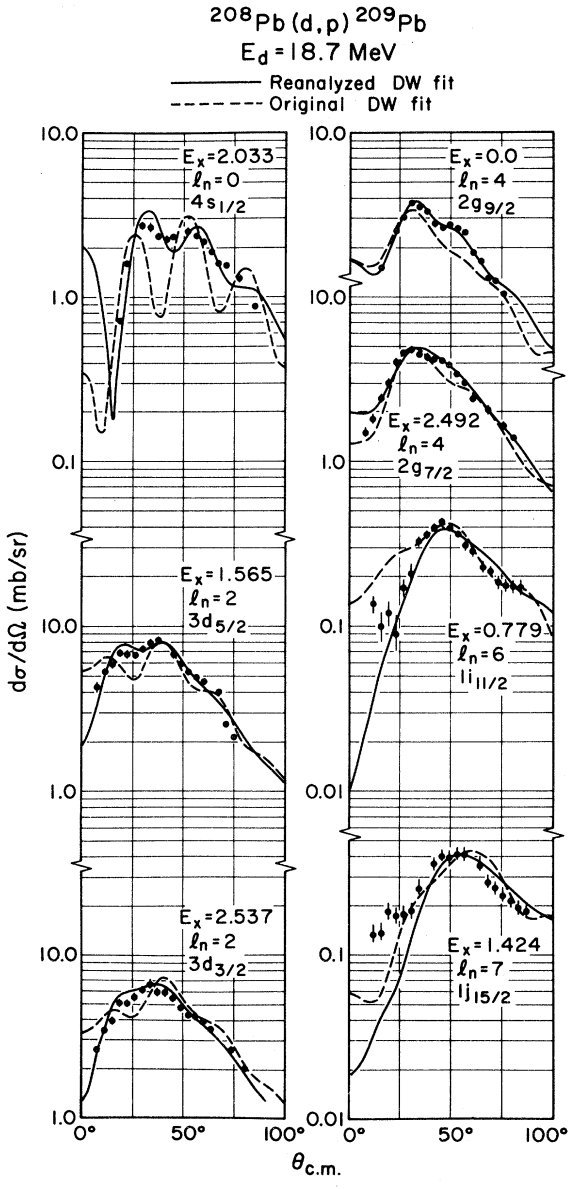

FIG. 4. The single-particle angular distributions of the ^{208}Pb$(d,p)^{209}$Pb reaction at 18.7 MeV incident energy as originally fitted and as now reanalyzed. The data are from Ref. 19.

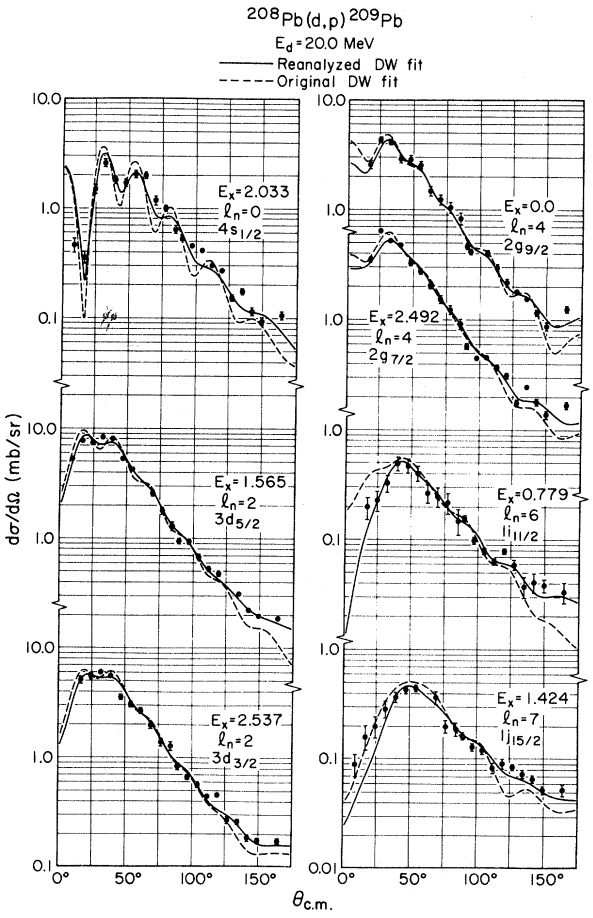

FIG. 5. The single-particle angular distributions of the ^{208}Pb$(d,p)^{209}$Pb reaction at 20.0 MeV incident energy. The data are from Ref. 21.

^{209}Pb single-particle transitions taken at $E_d = 13.0$ MeV.

The reanalysis of all this older data and our own new data was accomplished with the use of the neutron, deuteron, and proton parameter sets given in Table II. The bound state of the captured neutron was approximated by an eigenfunction of a central Woods-Saxon potential (with a spin-orbit term) whose depth was adjusted to give the observed binding energy of the level. With the exception of the 20.0 MeV deuteron parameter set, the optical-model potentials listed were determined conventionally, i.e., these parameters will fit the elastic scattering angular distributions. The two 13.0 MeV sets are similar to those discussed by Casten *et al.*[22] in their 12.3 and 15.0 MeV ^{208}Pb$(\vec{d},p)$ studies. With the sets designated PE and PE1, these authors were able to fit the ^{209}Pb single-particle angular distributions and polarizations, in addition obtaining spectroscopic strengths near unity (except for the $1j_{15/2}$). For our 20.0 MeV data analysis, the proton optical potential was that derived by Satchler[11] and is based on fits to the elastic proton scattering cross sections and polarizations on ^{208}Pb at 19.0, 20.0, 25.0, and 30.0 MeV incident energy. Also in the literature is a set proposed by Perey[9] in 1964, based on 17.0 MeV scattering from ^{208}Pb. The two sets differ mainly in the depth of the imaginary absorption term, 7.5 MeV for the Perey set and 10.0 MeV for the Satchler set. The discrepancy can be explained by noting that 17.0 MeV cor-

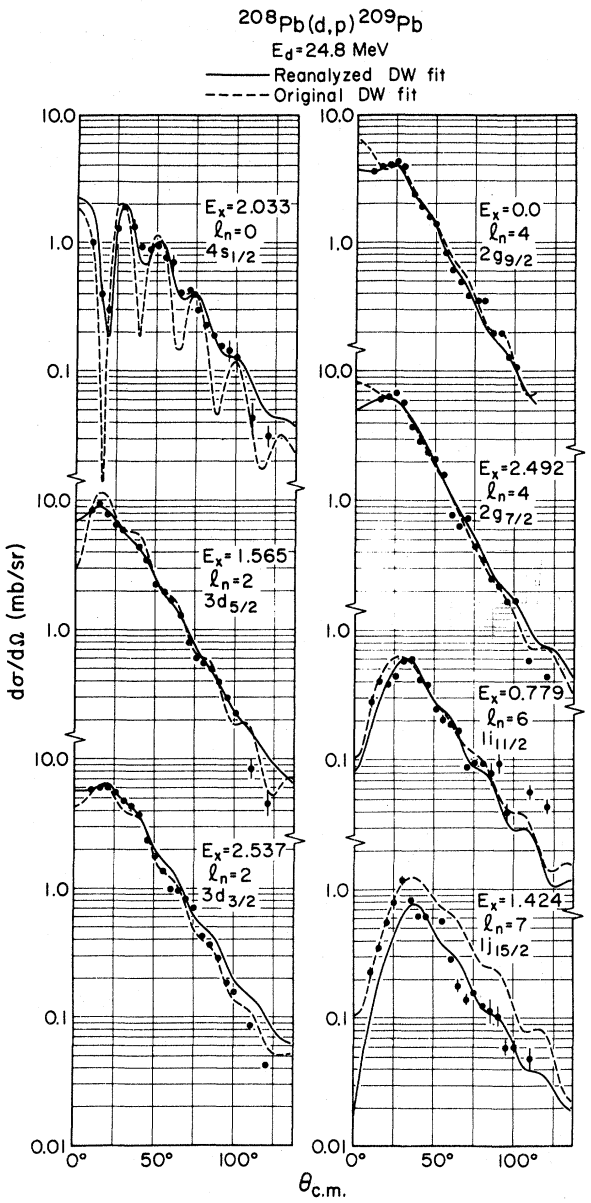

FIG. 6. The single-particle angular distributions of the ^{208}Pb$(d,p)^{209}$Pb reaction at 24.8 MeV incident energy. The data are from Ref. 10.

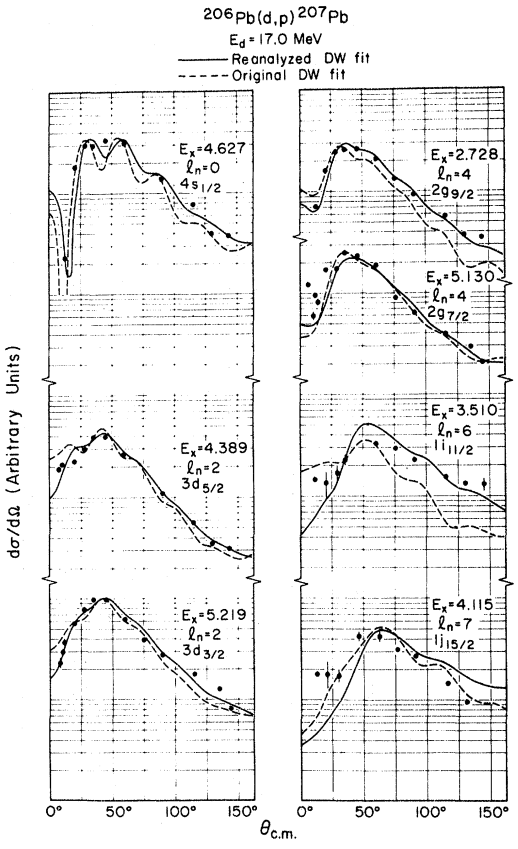

FIG. 7. The main fragments in the ^{206}Pb$(d,p)^{207}$Pb reaction with their angular distributions. At 17.0 MeV incident energy, only the $2g_{9/2}$ and $1i_{11/2}$ groups are outside the resonance region. The data are from Ref. 5.

responds to a resonance (the $4s_{1/2}$, and, at 17.4 MeV, the $2g_{7/2}$-$3d_{3/2}$) in the elastic channel,[1] violating the fundamental basis of the optical model. The increased elastic channel flux from this resonance has the effect of reducing the absorption depth from what it would normally be. Thus, the use of this Perey set should be avoided. The existence of the isobaric analog resonances in the elastic proton channel also complicates the analyses of direct reactions in the lead region for proton energies between 15.0 and 17.5 MeV. For example, anomalies generally appeared in (d,p) and (p,d) excitation functions whenever the proton is in this energy range.[23] Tamura and Coker[24] propose an explanation of these anomalies, quantitatively and qualitatively, in the context of the shell-model approach to reaction theory. This approach results in the use of a resonating transition amplitude in addition to the normal DWBA amplitude. We thus are of the opinion that our straightforward analysis of the 13.0 MeV hole-state angular distributions for ^{205}Pb ($E_p = 15 \rightarrow 17.5$ MeV) may be incorrect in an amount difficult to determine. This difficulty does not apply to the analysis of the 20.0 MeV data for which the proton groups are far above the resonance region.

The remaining parameter set of Table II, that for the 20.0 MeV deuterons, is cited as case No. 3 in Ref. 11. It is not a conventional optical-model parameter set. Instead a parameter set based on the Johnson-Soper deuteron breakup model[13] was used to generate the deuteron relative motion function. Following the Johnson-Soper method, Satchler[11] has been able to fit the ^{208}Pb$(p,d)^{207}$Pb angular distributions without the use of radial cutoffs in the transition matrix element. However, it should be noted that the lower angular momentum (l_n) transfers are least affected by the choice be-

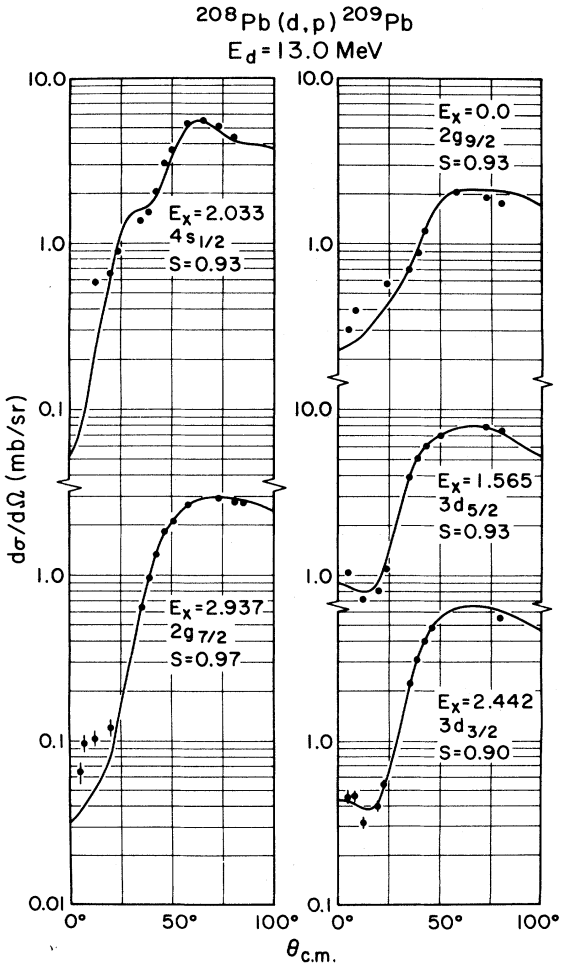

FIG. 8. Fits to the ^{208}Pb$(d,p)^{209}$Pb single-particle angular distributions at $E_d = 13.0$ MeV. A combination of contaminant interferences and intrinsic weakness rendered the $1i_{11/2}$ and $1j_{15/2}$ angular distributions nonsignificant in the angles exposed (5°→80°).

TABLE II. Optical parameters used in distorted-wave analysis. Optical potentials are of a Woods-Saxon form with V_0 a real volume term of radius $r_0 A^{1/3}$ and diffuseness a; W' is an imaginary surface absorption; V_{so} is a real surface spin-orbit potential. The values for W' and V_{so} given here include the factor of 4.0 required by DWUCK.

Incident energy (MeV)	Particle	V_0 (MeV)	r_0 (fm)	a (fm)	W' (MeV)	r_0' (fm)	a' (fm)	V_{so} (MeV)	r_{so} (fm)	a_{so} (fm)	r_c (fm)
13.0	d	106.0	1.15	0.981	82.0	1.34	0.68	28.0	1.15	0.81	1.30
	p	58.0	1.25	0.65	54.0	1.25	0.47	30.0	1.25	0.65	1.25
20	d	112.0	1.25	0.682	77.6	1.25	0.783	24.0	1.12	0.47	1.30
	p	52.0 [a]	1.25	0.65	40.0	1.25	0.76	24.0	1.12	0.47	1.25
13 and 20.0	n	b	1.25	0.65				($\lambda = 25$) [c]			

[a] Satchler (Ref. 11) gives the formula $V_0(\text{MeV}) = 58.4 - 0.3E_p$ for the real depth of the proton well. The value 52.0 MeV represents a convenient average for the range of proton energies covered.

[b] Depth adjusted until the binding well reproduced the given level's experimental separation energy.

[c] The spin-orbit term of the form factor potential is equal to λ times the Thomas term.

tween the conventional and breakup parameter sets, so that for $l_n \leq 3$, these results are not sensitive to the correctness of the deuteron breakup model compared to the conventional optical model.

The spectroscopic factors derived from the reanalysis of the ^{208}Pb(d,p) data using the 20 MeV potentials are listed here in Table III. It is pointed out that except for the $2g_{9/2}$ and $1i_{11/2}$ transfers, the single-particle transfers effected at 17.0 deuteron energy result in outgoing protons in the analog-resonance energy range. In particular, the $1j_{15/2}$ fragment in ^{207}Pb is reported by Moyer *et al.*[5] to have 40% *more* spectroscopic strength than the main fragment in ^{209}Pb. This seems highly unlikely, since one would expect a splitting rather than a fusion of spectroscopic strength as one moves away from ^{209}Pb. Indeed it will be seen here that the main $1j_{15/2}$ fragment in ^{205}Pb (measured at two "nonresonant" incident energies) has only about half the strength of the ^{209}Pb state. Assuming no doublet to be involved, it may be that the resonance in the proton channel is affecting the 17.0 MeV (d,p) analysis. Other than the higher-lying states excited at $E_d = 17.0$ MeV, the only other major discrepancy indicated in Table III is that for the $2g_{9/2}$ transfer at $E_d = 24.8$ MeV in which both the original and the reanalyses give a spectroscopic factor of 0.67. This failure is somewhat surprising, since the reanalysis has generated a significantly improved fit to the stripping peak in the angular distribution (Fig. 6). We would point out, however, that the Muehllehner *et al.*[10] study was part of a systematic analysis at $E_d = 14.8$ and 20.1 MeV. Kovar[21] in his 20.0 MeV study has found a 20% discrepancy in the absolute cross section for the $2g_{9/2}$ transfer as measured in his and the Muehllehner work. The direction of the error, assuming it was in Muehllehner's measurement and carried over into the 24.8 MeV study, would serve to increase the observed spectroscopic strength to a value closer to unity. Neglecting these two areas of discrepancy it can be said that the reanalysis has provided generally improved fits to the ^{209}Pb angular distributions as well as a more consistent set of spectroscopic factors.

Spectroscopic factors for the new 13.0 MeV data are listed on Fig. 8. At this energy the protons populating the ground state may be affected by the $g_{9/2}$ resonance (see Fig. 1); however, the S_{lj} for the five single-particle states observed are all of the order of unity. Further detail on the comparison between the original and the revised fits may be found in Ref. 16. The net result is that the DWBA method appears to be quite reliable in the lead region (±15%) and there should be no need to distinguish between normalizing the ^{205}Pb cross sections to ^{209}Pb, or, more conventionally, comparing the ^{205}Pb predicted angular distributions to those experimentally observed.

TABLE III. Spectroscopic factors from earlier ^{208}Pb$(d,p)^{209}$Pb experiments.

	17.0 MeV [a]		18.7 MeV [b]		20.0 MeV [c]		24.8 MeV [d]	
nlj	Orig.	Refit	Orig.	Refit	Orig.	Refit	Orig.	Refit
$2g_{9/2}$	0.68	0.92	0.66	0.92	0.83 (0.72)	0.92	0.67	0.67
$1i_{11/2}$	0.81	1.10	0.75	1.10	0.86 (0.83)	1.14	0.94	0.89
$1j_{15/2}$	0.39 [e]	0.57 [e]	0.71	0.78	0.58 (0.47)	0.77	1.13 [f]	0.77 [f]
$3d_{5/2}$	0.65 [e]	0.75 [e]	0.62	1.00	0.98 (0.88)	0.89	1.00	0.92
$4s_{1/2}$	0.52 [e]	0.56 [e]	0.70	0.93	0.98 (0.95)	0.85	0.93	1.10
$2g_{7/2}$	0.93 [e]	1.05 [e]	0.81	0.92	1.05 (0.95)	0.95	1.17	0.90
$3d_{3/2}$	1.13 [e]	1.23 [e]	0.88	1.00	1.07 (0.90)	0.99	1.17	1.07

[a] Reference 5.
[b] Reference 19.
[c] Reference 21. The numbers in parentheses refer to the fits obtained using conventional deuteron parameters and the Perey 17.0 MeV proton optical parameter set.
[d] Reference 10.
[e] The outgoing protons from these residual states are within the elastic proton resonance region ~14.5 → 17.5 MeV.
[f] Unacceptable fit to the experimental shape makes this value questionable.

IV. ^{205}Pb RESULTS

The optical-model parameters, which in the previous section are shown to yield improved analyses of the ^{208}Pb data, were used to predict angular distributions for the ^{204}Pb(d,p) data obtained with 20.0 MeV deuterons. The 13.0 MeV data analysis need not be so involved as the 20.0 MeV analysis. The energies of the proton groups corresponding to states with $E_{ex}>2.75$ MeV are below the first analog resonance and the incoming 13.0 MeV deuterons, according to the breakup model, may be treated with a normal optical parameter set. [The ground-state Q value for ^{205}Pb is 4.510 MeV (Nuclear Data Sheets, 1960). The first particle state (2.565 MeV) corresponds to a proton energy of 14.72 MeV c.m. compared with 14.86 MeV for the $2g_{9/2}$ resonance in the $p+^{208}$Pb experiment.] Since their incident energy is near the Coulomb barrier, the 13.0 MeV deuterons are not affected by the nuclear field of the target as much as the 20.0 MeV deuterons. The optical parameter sets used for the 13.0 and the 20.0 MeV data analyses are given in Table II.

The spectroscopic factors S_{lj} listed in Table I are the weighted averages derived from analyses of both the 13.0 and the 20.0 MeV data. The errors ΔS_{lj} are based on the scatter of individual determination at each angle, and are assigned solely from consideration of the fitting errors, the scanning errors, and the errors in estimating background.

In Figs. 9 and 10 are shown fits to the strongest

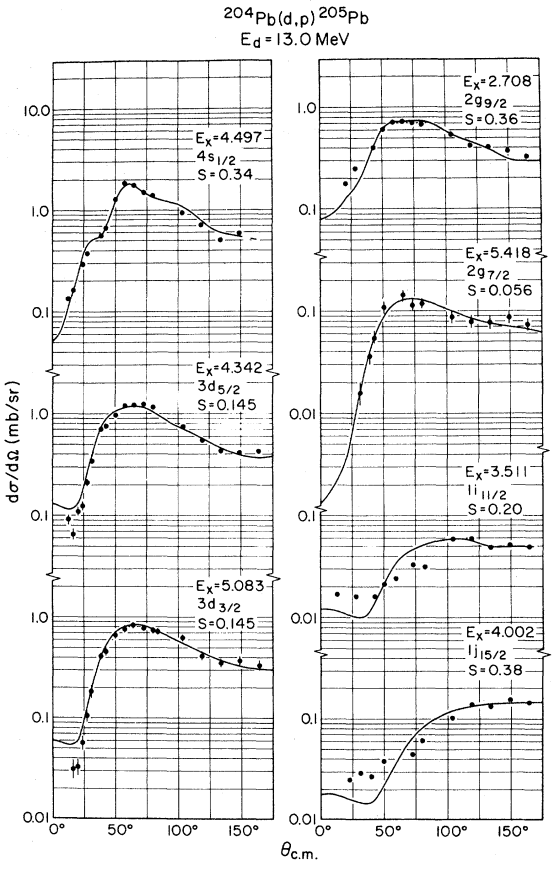

FIG. 9. Fits to the strongest different particle-state fragments of the ^{204}Pb$(d,p)^{205}$Pb reaction at $E_d=13.0$ MeV.

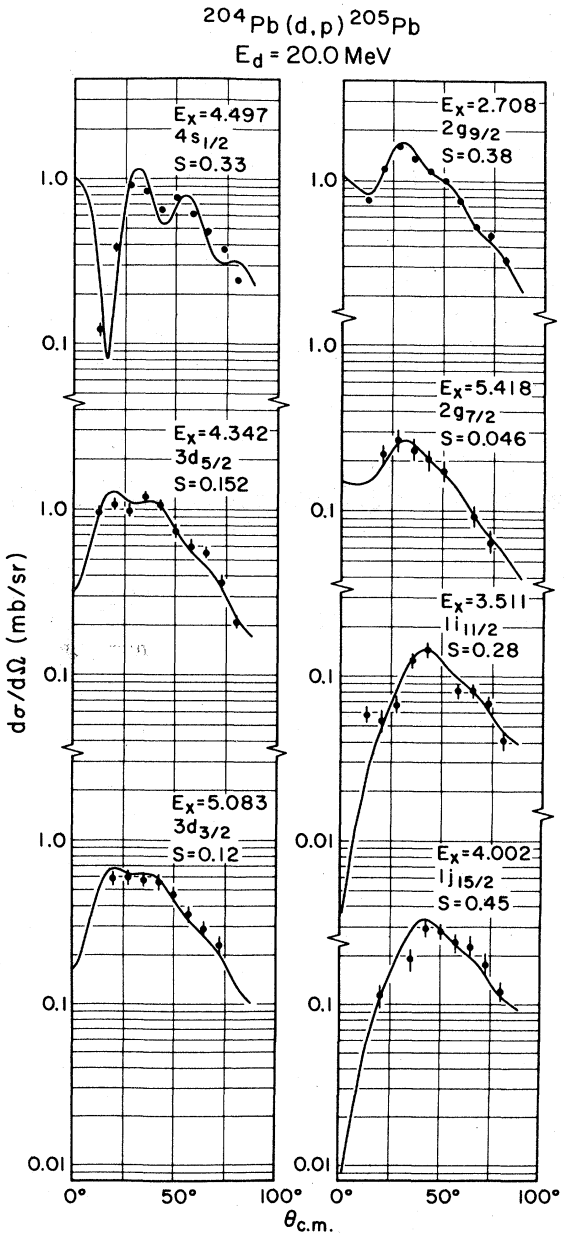

FIG. 10. Fits to the strongest different particle-state fragments of the ^{204}Pb$(d,p)^{205}$Pb reaction at $E_d=20.0$ MeV.

shell-model fragments in ^{205}Pb as observed at $E_d = 13.0$ and 20.0 MeV, respectively. For comparison the fits to the single-particle states in ^{209}Pb can be seen in Figs. 8 and 5. Although these fits are quite good, they are not by themselves conclusive. In similar experiments on ^{206}Pb [5] and on ^{202,204}Hg [25] at one incident energy, Moyer had great difficulty in distinguishing between the $2g_{7/2}$ and $3d_{3/2}$ transfer shapes. In the present work, for which two incident energies are employed, it becomes much easier to discriminate between the different angular momentum transfers. This is so because (for the range of values pertinent here) as one goes from a lower to a higher incident energy, the cross section for a larger l_n transfer increases with respect to that for a smaller l_n transfer. Table IV demonstrates this effect using the experimental maxima of the differential cross section for ^{208}Pb$(d,p)^{209}$Pb at $E_d = 13.0$ and 20.0 MeV. Hence, if the $2g_{7/2}$ state were misassigned as the $3d_{3/2}$ state in the 13.0 MeV analysis, its spectroscopic factor at 20.0 MeV would be 2.25 times as large as at 13.0 MeV. In anticipation of the results to be described for ^{205}Pb, the last column of Table IV notes that binding-energy differences of a few hundred keV are not expected to alter the intensity ratios significantly. In this manner all the l_n assignments of the ^{205}Pb states in Table I were checked. Such a procedure of course, does not resolve the general total spin ambiguity ($j = l_n \pm \frac{1}{2}$) common to all unpolarized experiments. In reality, though, there is really only one serious j-value ambiguity in ^{205}Pb in the seven orbits of Table IV. The polarization data of Casten *et al.*[22] and the ^{205}Bi decay studies of Hamilton *et al.*[26] and of Rupp and Vegors[27] have established a $\frac{9}{2}^+$ assignment for the strongest $2g_{9/2}$ fragments (Nos. 1, 2, and 5 of Table I). There is, of course, no ambiguity for the $4s_{1/2}$ and the $1j_{15/2}$ fragments, and because of sum-rule limits there is very little ambiguity for the $1i_{11/2}$ and the $2g_{7/2}$ states. Thus, only the distinction between the $3d_{5/2}$ and the $3d_{3/2}$ fragments can be reasonably questioned. Figure 11 presents the strongest ($S_{lj} > 0.015$) particle-state fragments as they are assigned in Table I. In the context of the entire spectrum it can be seen that the assignments which were made are the most probable. Overall, unless one is willing to argue for an inversion of the $3d_{3/2}$ and $3d_{5/2}$ fragments, or, less drastically, for an arbitrary interweaving of these fragments, it must be concluded that there is a concentration of spectroscopic strength in ^{205}Pb rather narrowly about the centroids. This is especially true for the $2g_{9/2}$ and $4s_{1/2}$ orbitals, and, although less dramatic, is still recognizable for the $2g_{7/2}$ orbital. In this respect, the simple shell-model potential (central field plus spin-orbit term) clearly predominates over the smearing effects of the residual interaction.

The only theoretical calculation for the ^{205}Pb particle states was done by Rao[7] who used a particle-vibration model form of the residual interaction to predict the spectrum. This predicted spectrum is found to be in substantial variance with the experimental spectrum of ^{205}Pb. For example, the main $2g_{9/2}$ strength is given by Rao in one state at 0.9 MeV whereas in fact the main strength is distributed over three closely lying levels above 2.565 MeV. Within the framework of

TABLE IV. The maxima of the (d,p) differential cross sections at 13.0 and 20.0 MeV incident energy.

nlj	E_B^{209} [a] (MeV)	$(d\sigma/d\Omega)_{max}$ [b] (mb/sr) 13.0 MeV	20.0 MeV	Ratio	E_B^{205} [a] (MeV)	(Ratio)′ [c]
$2g_{9/2}$	−3.945	2.03	4.40	2.17	−4.038	2.14
$1i_{11/2}$	−3.146	0.19	0.50	2.63	−3.242	2.58
$1j_{15/2}$	−2.511	0.13 [d]	0.45	3.46	−2.733	3.23
$3d_{5/2}$	−2.380	7.90	8.40	1.06	−2.571	1.11
$4s_{1/2}$	−1.912	5.45	2.60	0.48	−2.193	0.50
$2g_{7/2}$	−1.450	2.87	6.45	2.25	−1.443	2.25
$3d_{3/2}$	−1.405	6.09	6.10	1.00	−1.675	1.07

[a] Binding energy of the single-particle state in ^{209}Pb, or (in column 6) the fragments' centroid in ^{205}Pb.

[b] The maximum of the differential cross section ^{208}Pb$(d,p)^{209}$Pb as experimentally observed at these incident energies (see Figs. 10 and 5).

[c] The experimental ratios for ^{209}Pb multiplied by the Q-value corrections calculated using the optical parameters in Table II.

[d] The $1j_{15/2}$ transfer is predicted to peak at far back angles at which plates were not exposed. The value quoted here is that based on the shape of the DWBA curve as normalized to the forward angle data points.

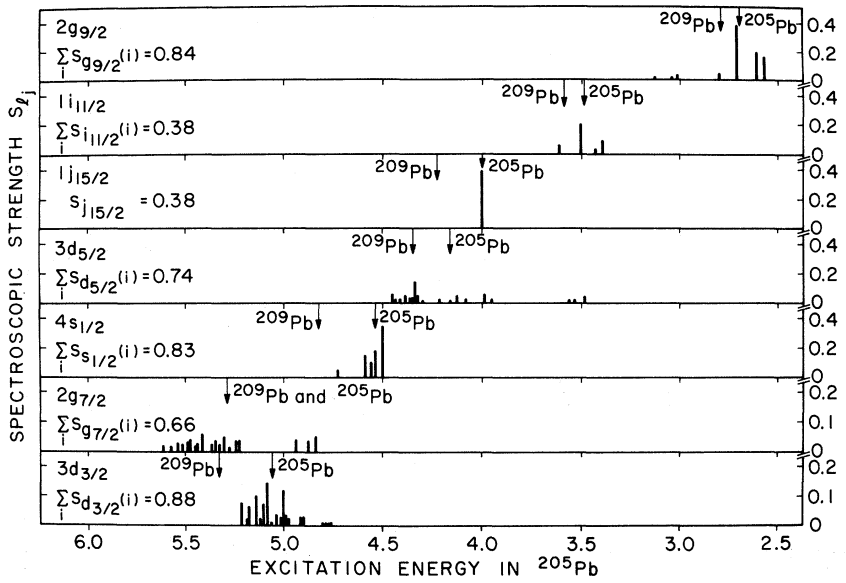

FIG. 11. The spectroscopic strength distribution for the particle states in ^{205}Pb. The arrows denote the positions of the ^{205}Pb centroids and the corresponding single-particle states in ^{209}Pb.

the particle-vibration model we suggest that a scheme for generating a triplet of $2g_{9/2}$ fragments, as shown in Fig. 12, is possible. The arguments for this scheme are based entirely on the branching ratios for ^{205}Pb decays which can be obtained from the data presented by Hamilton *et al.*[26] For example, the $\frac{7}{2}^-$ 0.703 MeV state is observed to decay almost entirely (E_2) to the $\frac{5}{2}^-$ ground state, while a similarly allowed decay to the $\frac{3}{2}^-$ state at 0.262 MeV cannot be seen. In addition, the 0.703 MeV state cannot be seen in either neutron stripping or pickup reactions, implying that the state cannot be represented simply as a particle (hole) coupled to ^{204}Pb (^{206}Pb). Instead the state may be based on the excited 2^+ core as both Miranda[28] and Rao[7] have suggested. In that case the overwhelming decay to the ground state may be simply interpreted as the excited core state decaying to the 0^+ state, leaving the $2f_{5/2}$ neutron as a spectator. Following this line of reasoning, it is noted that the strongest branches out of the first two $2g_{9/2}$ states are to this 0.703 MeV state. In this regard, we hypothesize that the configuration $|^{204}\mathrm{Pb}^{3^-}_{2.62} \otimes 2f_{5/2}(0.0\ \mathrm{MeV})\rangle_{9/2^+}$ is admixing with the shell-model configuration $|^{204}\mathrm{Pb}^{0^+}_{g.s.} \otimes 2g_{9/2}\rangle_{9/2^+}$, a not unlikely event in view of the near degeneracy in energy. In that case, the excited 3^- core simply $E1$ decays to the excited 2^+ core of the 0.703 MeV state. Finally, a third configuration $|^{204}\mathrm{Pb}^{4^+}_{1.27} \otimes 1i_{13/2}(1.01\ \mathrm{MeV})\rangle_{9/2^+}$ can admix with the other two to produce the observed triplet. Although the energy denominator involved in this mixing is not as favorable, it is noted that the $2g_{9/2}$ fragments display a relatively large $E2$ decay to the $\frac{13}{2}^+$ state at 1.014 MeV, consistent with our scheme. It is possible then, that a coupling parameter different from the one that Rao used ($\eta = 0.30$) will, in conjunction with the configurations proposed here, produced a better predicted spectrum for ^{205}Pb.

Even without a detailed knowledge of the origins of the splittings, very interesting trends emerge when the fragmentations in ^{205}Pb and in ^{207}Pb are compared. In ^{207}Pb at least 50% of the expected spectroscopic strength is to be found in a single state for the $2g_{9/2}$, $3d_{5/2}$, $4s_{1/2}$, and the $3d_{3/2}$ orbitals. No such concentration of strength appears in ^{205}Pb but the least fragmented orbitals in ^{207}Pb (the $2g_{9/2}$ and the $4s_{1/2}$) are the same as those in ^{205}Pb. Likewise, the most fragmented state, the $2g_{7/2}$, also displays the most pronounced smearing in ^{205}Pb.

Another persisting trend is that of the centroid binding energies for ^{209}Pb, ^{207}Pb, and ^{205}Pb as listed in Table V. The $4s_{1/2}$, $3d_{3/2}$, $3d_{5/2}$, and $1j_{15/2}$ states show a marked increase in binding energy in going from ^{209}Pb to ^{205}Pb, while on the other hand the $2g_{7/2}$ and the $2g_{9/2}$ states are much less affected. We initially realized that a deformed nucleus with a Dl^{-2} term in the potential might explain the depression of the highest l_n state ($1j_{15/2}$) and the lack of movement of the $l_n = 4$ states. Bromley[29] has also pointed out that behavior of the remaining states is understandable if one assumes that the macroscopic nuclear potential in ^{205}Pb is more diffuse than that in ^{209}Pb. The lowest l_n orbits have the highest number of radial nodes and thus in ^{205}Pb with a more diffuse

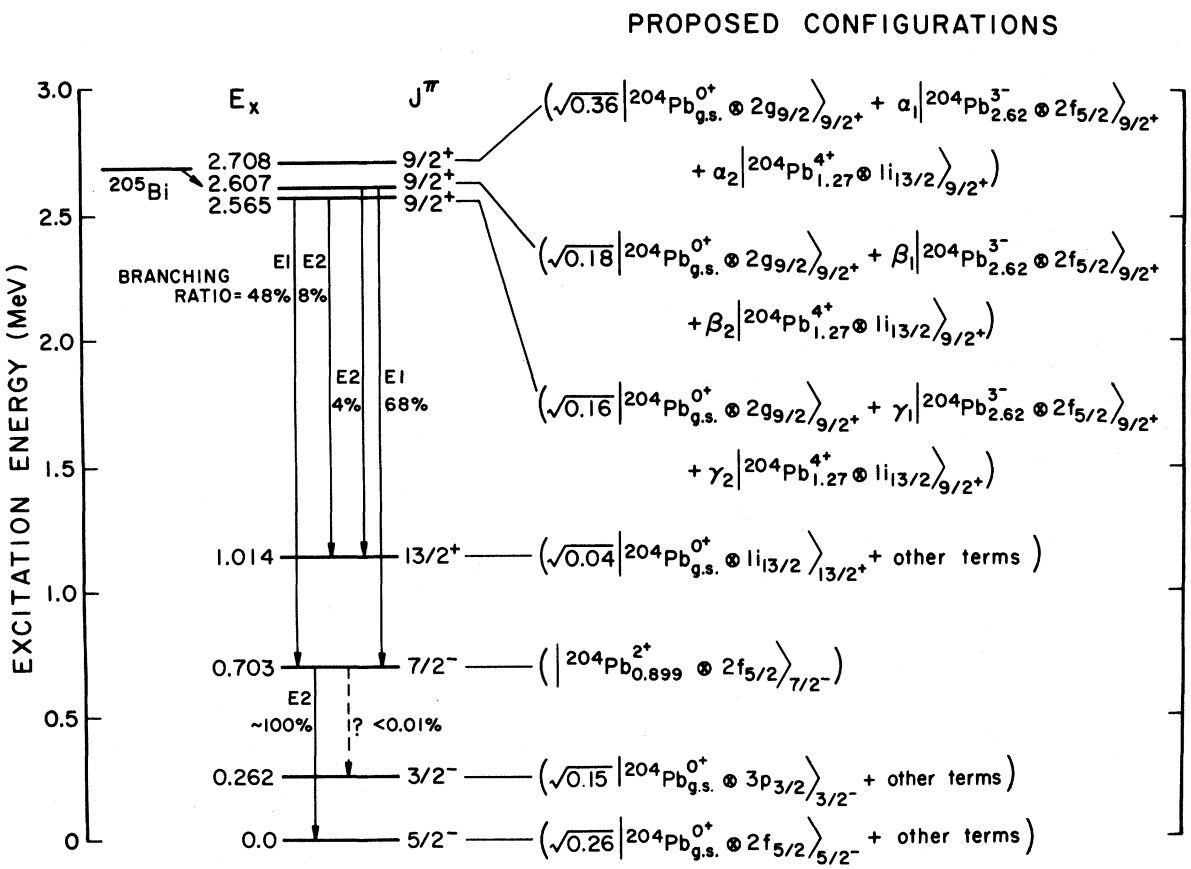

FIG. 12. Evidence for a particle-vibration description of the splitting of the $2g_{9/2}$ orbit in ^{205}Pb. The remaining de-excitation out of the 2.565 and 2.607 MeV states goes to a number of omitted levels. Moreover, there are weak $E3$ branches directly to the ground state whose mere existence argues for collectivity in the $\frac{9^+}{2}$ states.

potential, these orbits would become more bound. In any case the ordering of the $2g_{7/2}$ and the $3d_{3/2}$ orbitals in ^{209}Pb is reversed in ^{205}Pb.

V. CONCLUSIONS

This paper and that immediately preceding report comprehensive examination of the excitation spectrum of ^{205}Pb as probed by the (d,p) reaction. Not only has it been possible to reach conclusions concerning the nuclear structure of this three-hole nucleus, but also we have been able to revise substantially previous conclusions regarding the reaction calculation itself. That is, the (d,p) angular distributions in the lead region can be much better predicted by the DWBA method than earlier studies have indicated. This improvement has been achieved through a better approximation of the optical potentials describing the in-

TABLE V. Binding energies of the single-particle states in the odd Pb nuclei.

nlj	^{209}Pb (MeV)	^{207}Pb (MeV)	^{205}Pb (MeV)
$2g_{9/2}$	−3.944	−3.978	−4.038
$1i_{11/2}$	−3.165	−3.223[a]	−3.242[a]
$1j_{15/2}$	−2.502	−2.618	−2.733[a]
$3d_{5/2}$	−2.379	−2.431	−2.572
$4s_{1/2}$	−1.911	−2.085	−2.193
$2g_{7/2}$	−1.452	−1.466[a,b]	−1.443
$3d_{3/2}$	−1.407	−1.526	−1.675

[a] More than half the expected single-particle strength is missing.

[b] The difficulties experienced by Moyer *et al.* (Ref. 5) in distinguishing $g_{7/2}$ and $d_{3/2}$ transfers make this value questionable. Since there is more unassigned $2g_{7/2}$ strength than missing $3d_{3/2}$ strength, the centroid energy quoted here assumes two other states in ^{207}Pb are actually $2g_{7/2}$ in addition to the only definitely assigned $\frac{7}{2}$ state at $E_B = 1.611$ MeV.

coming deuteron and the outgoing proton channels.

In both the low-lying and the higher-lying excitation regions a clear concentration of the available spectroscopic strength about its centroid is demonstrated. This observation is illustrated in Fig. 13, describing the strength distributions in terms of two parameters $\Gamma_{2/3}$ and $N_{2/3}$. The number $N_{2/3}$ is the minimum of states accounting for $\frac{2}{3}$ of the observed spectroscopic strength for a given orbital. The parameter $\Gamma_{2/3}$ is the width (in MeV) spanned by the states included in $N_{2/3}$. Although somewhat arbitrary, the pattern exhibited by these parameters is clearly a consequence of the persistence of simple shell-model behavior in ^{205}Pb. No one calculation has yet attempted to reproduce or predict the entire ^{205}Pb spectrum, that is, both the one-particle four-hole states and the three-hole states. While it would undoubtedly be complex, it would be important to undertake such an effort in light of the data presented here.

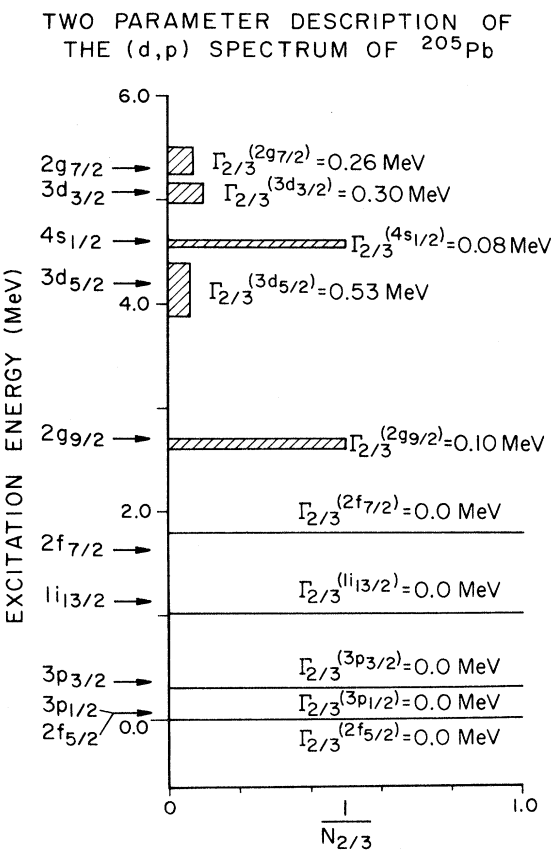

FIG. 13. Two-parameter condensation of the (d,p) excitation spectrum of ^{205}Pb.

ACKNOWLEDGMENTS

In addition to the fine technical support offered by Edmond Comeau, Charles Gingell, and the accelerator crew, we record our thanks for the patient and careful scanning of the photographic plates by Bernadette Kennedy and Muriel Wright. The support and interest of Professor D. A. Bromley and Professor P. D. Parker is greatly appreciated.

*Work supported by U.S.E.R.D.A. Contract E(11-1)-3074.

†Present address: Physics Department, Vanderbilt University, Nashville, Tennessee 37235.

‡Present address: Argonne National Laboratory, Argonne, Illinois 60439.

§Present address: Malden Public School System, Malden, Massachusetts 02148.

[1]N. Stein, in *Proceedings of the International Conference on the Properties of Nuclear States, Montreal, 1969*, edited by M. Harvey *et al.* (Univ. of Montreal Press, Montréal, Canada, 1969).

[2]N. Stein, in *Nuclear Isospin*, edited by J. D. Anderson (Academic, New York, 1969), pp. 481–534.

[3]D. Bromley and J. Weneser, Comments Nucl. Part. Phys. 11, 51 (1968).

[4]E. Ayoub, R. Ascuitto, and D. A. Bromley, Phys. Rev. Lett. 29, 182 (1972).

[5]R. Moyer, B. Cohen, and R. Diehl, Phys. Rev. C 2, 1898 (1970).

[6]P. Mukherjee, K. V. Chalapati Rao, and I. Mukherjee, Nucl. Phys. A129, 535 (1969).

[7]K. V. Chalapati Rao, Nucl. Phys. A166, 213 (1971).

[8]M. Macfarlane, in *Proceedings of the International Conference on the Properties of Nuclear States, Montreal, 1969* (see Ref. 1).

[9]F. Perey, in Nuclear Spectroscopy with Direct Reactions, edited by F. Throw [ANL Report No. ANL-6848, 1964 (unpublished)], p. 114.

[10]G. Muehllehner, A. Poltorak, W. Parkinson, and R. H. Bassel, Phys. Rev. 159, 1039 (1967).

[11]G. Satchler, Phys. Rev. C 4, 1485 (1971).

[12]J. Harvey and R. Johnson, Phys. Rev. C 3, 636 (1971).

[13]R. Johnson and P. Soper, Phys. Rev. C 1, 976 (1970).

[14]D. Bouldin and F. Levin, Nucl. Phys. A189, 449 (1972).

[15]P. Spink and J. Erskine, Argonne National Laboratory Physics Division Informal Report No. PHY-1965B, 1965 (unpublished).

[16]C. Maguire, Ph.D. thesis, Yale University, 1973 (unpublished).

[17]P. D. Kunz (private communication).

[18]J. Ungrin, R. Diamond, P. Tjøm, and B. Elbek, K. Dansk. Vidensk. Selsk. Mat-Fys. Medd. 38, No. 8 (1971).

[19]A. Jeans, W. Darcey, W. Davies, and P. Smith, Nucl. Phys. A128, 224 (1969).

[20]F. Perey, Phys. Rev. 131, 745 (1963).

[21]D. G. Kovar, Ph.D. thesis, Yale University, 1970 (unpublished). The present revision was incorporated in Table 3 and Fig. 9 of D. G. Kovar, N. Stein, and C. K. Bockelman, Nucl. Phys. A231, 266 (1974).

[22]R. Casten, E. Cosman, E. Flynn, O. Hansen, P. Kea-

ton, N. Stein, and R. Stock, Nucl. Phys. A202, 161 (1973).
[23]N. Stein, J. P. Coffin, C. Whitten, and D. Bromley, Phys. Rev. Lett. 21, 1456 (1968).
[24]T. Tamura and R. Coker, Phys. Lett. 30B, 581 (1969).
[25]R. Moyer, Phys. Rev. C 5, 1678 (1972).
[26]J. Hamilton, V. Ananthakrishnan, A. V. Ramayya, W. M. LaCasse, D. C. Camp, J. J. Pinajian, L. H. Kern, and J. C. Manthuruthil, Phys. Rev. C 6, 1265 (1972).
[27]T. Rupp and S. Vegors, Nucl. Phys. A163, 545 (1971).
[28]A. Miranda, Nucl. Phys. A92, 386 (1967); also C. Riedel, R. Broglia, and A. Miranda, Nucl. Phys. A113, 503 (1968).
[29]D. A. Bromley (private communication).